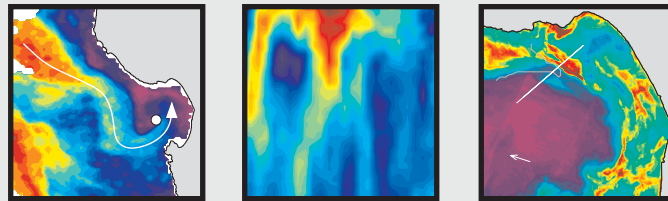


COASTAL OCEAN PHYSICS and RED TIDES

AN EXAMPLE FROM
MONTEREY BAY, CALIFORNIA

BY JOHN P. RYAN, HEIDI M. DIERSSEN, RAPHAEL M. KUDELA,
CHRISTOPHER A. SCHOLIN, KENNETH S. JOHNSON,
JAMES M. SULLIVAN, ANDREW M. FISCHER, ERICH V. RIENECKER,
PATRICK R. MCENANEY, AND FRANCISCO P. CHAVEZ



Dense accumulations of certain phytoplankton make the ocean appear reddish. Some of these “red tides” poison marine life and negatively impact coastal fisheries and human health. Complex variability in coastal waters coupled with rudimentary understanding of phytoplankton ecology challenge our ability to understand and predict red tides. During fall 2002, multi-scale physical and biological observations were made preceding and during a red tide bloom in Monterey Bay, California. These intensive observations provided insight into the physical oceanography underlying the event. The bloom was preceded by intrusion of a warm, chlorophyll-poor filament of the California Current, suddenly changing physical and biological conditions through most of the bay. Enhancement of vertical density stratification followed the intrusion and created conditions favoring dinoflagellates. Favorable environmental conditions led to red tide inception in the northern bay, and advection strongly influenced spread of the bloom throughout the bay and out into the adjacent sea. Concentration of dinoflagellates in convergence zones was indicated by the development of dense red tide patches in fronts and in wave-like aggregations having the same scale as internal waves that propagated through the bloom.

INTRODUCTION

Phytoplankton support most of the life in the ocean. However, some phytoplankton species can have deleterious impacts, primarily by producing toxins that are transferred to marine life and to people, by physically damaging or causing dysfunction of vital tissues (e.g., fish gills and skin), and by depletion of oxygen during respiration and decay of dense blooms (Glibert et al., introductory article, this issue). Blooms of these species are termed harmful algal blooms (HABs). Greater understanding of HABs is prompted not only by their impacts, but also by the apparent global increase in their occurrence (Hallegraeff, 2003). Red tides can, but do not always, cause harm; those that do are one category of HABs. Dinoflagellates constitute approximately 50 percent of all red tide species and 75 percent of all HAB species (Sournia, 1995; Smayda, 1997); therefore, di-

noflagellate ecology research is essential to advancing understanding of red tide and HAB phenomena. Among the most challenging aspects of this research is investigation of the physical oceanography that influences bloom initiation and development in complex, rapidly changing coastal environments (Tester et al., 1991;

Franks and Anderson, 1992; Anderson, 1995; Pitcher and Boyd, 1996; Donaghay and Osborn, 1997; Smayda, 2002).

Monterey Bay lies in the central California Current upwelling system (Figure 1) where phytoplankton productivity and abundance are greatly augmented by wind-driven upwelling of nutrient-rich

John P. Ryan (ryjo@mbari.org) is Scientist I, Monterey Bay Aquarium Research Institute, Moss Landing, CA, USA. **Heidi M. Dierssen** is Assistant Professor in Residence, University of Connecticut, Department of Marine Sciences, Groton, CT, USA. **Raphael M. Kudela** is Assistant Professor, University of California, Ocean Sciences Department, Santa Cruz, CA, USA. **Christopher A. Scholin** is Associate Scientist, Monterey Bay Aquarium Research Institute, Moss Landing, CA, USA. **Kenneth S. Johnson** is Senior Scientist, Monterey Bay Aquarium Research Institute, Moss Landing, CA, USA. **James M. Sullivan** is Marine Research Scientist, University of Rhode Island, Graduate School of Oceanography, Narragansett, RI, USA. **Andrew M. Fischer** is Research Technician, Monterey Bay Aquarium Research Institute, Moss Landing, CA, USA, and Ph.D. Candidate, Cornell University, Ithaca, NY, USA. **Erich V. Rienecker** is Research Technician, Monterey Bay Aquarium Research Institute, Moss Landing, CA, USA. **Patrick R. McEnaney** is Research Technician, Monterey Bay Aquarium Research Institute, Moss Landing, CA, USA. **Francisco P. Chavez** is Senior Scientist, Monterey Bay Aquarium Research Institute, Moss Landing, CA, USA.

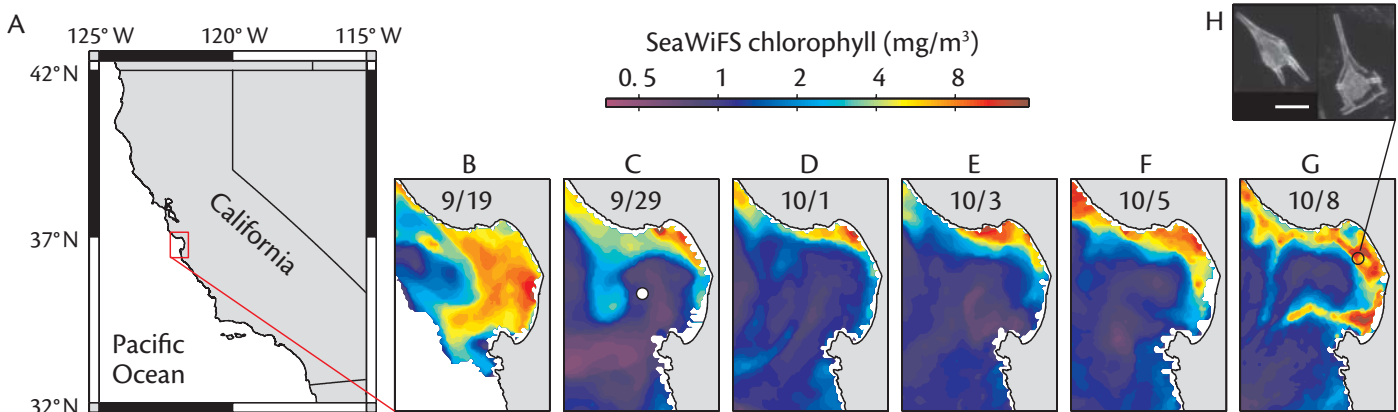


Figure 1. A red tide bloom following rapid environmental change in the central California Current (CC) upwelling system during late September to early October 2002. Near-surface chlorophyll concentrations in Monterey Bay and adjacent waters from the Sea-viewing Wide Field-of-view Sensor (SeaWiFS) satellite instrument illustrate flushing of the bay by a CC filament (B-D; see also Figure 2), and a red tide bloom that rapidly followed the flushing (E-G). Image spatial resolution is $\sim 1.1 \times 1.1$ km. The circle at the mouth of Monterey Bay in C shows the location of a mooring that provided measurements of water properties and ocean current velocities (Figure 3). The dinoflagellate species that dominated the bloom were (H) *Ceratium furca* (left) and *Ceratium dens*. The pictures are from a water sample taken on October 8, 2002, at the location indicated; the scale bar is 50 μm .

waters to the shallow sunlit layer (Ryther, 1969). Recent reviews frame the complex ecology of HABs in coastal upwelling systems (Smayda, 2000; Kudela et al., this issue). During a phytoplankton ecology research program in September and October of 2002, the bay experienced rapid changes in the physical environment and phytoplankton community. In 11 days, the bay changed from characteristic productive green-blue waters, to unproductive clear blue waters, and then to ruddy brown waters of a red tide that spread throughout the bay. Observed from the deck of a ship, the red tide was characterized by highly concentrated patches having sharp boundaries. The dinoflagellate species consistently found to dominate the red tide patches were *Ceratium furca* and *Ceratium dens* (Figure 1H), which are known to bloom in productive coastal waters of the Northeast Pacific (Horner et al., 1997; Smayda, 2002). Multidisciplinary, multi-scale observation of the bay and adjacent sea provided a lens through which red tide genesis and evolution were viewed.

METHODS

Satellite Remote Sensing

We obtained Level 1a Sea-viewing Wide Field-of-view Sensor (SeaWiFS) imagery and ancillary data required for their processing from the NASA/Goddard Distributed Active Archive Center (DAAC). The SeaDAS software was applied to atmospherically correct the imagery, compute chlorophyll concentration using the OC4v4 algorithm (O'Reilly et al., 1998), and geographically project the chlorophyll images. Mapped sea surface temperature (SST) imagery (Figure 2) was obtained from

the NOAA CoastWatch West Coast regional node. Synthetic aperture radar (SAR) imagery was obtained from the Alaska Satellite Facility (ASF) and was projected from satellite to map coordinates using software from ASF.

Aircraft Remote Sensing

On October 7, the Airborne Visible/Infrared Imaging Spectrometer (AVIRIS) imaged the bay and adjacent waters in 51 minutes with four parallel swaths, each 11 km wide and overlapping by 1 km. Sun glint was avoided by orienting flight line headings toward the sun.

The AVIRIS imagery was atmospherically corrected using an algorithm developed for hyperspectral remote sensing (Gao et al., 2000; Montes et al., 2004). Atmospheric correction results were validated with reflectance spectra computed from optical measurements of the ocean surface, the sky, and a reference Kodak gray card. These measurements were made using a HOBI Labs HydroRad hyperspectral radiometer during the AVIRIS acquisition. Chlorophyll concentration was computed from the atmospherically corrected image spectra using the SeaWiFS OC4v4 algorithm.

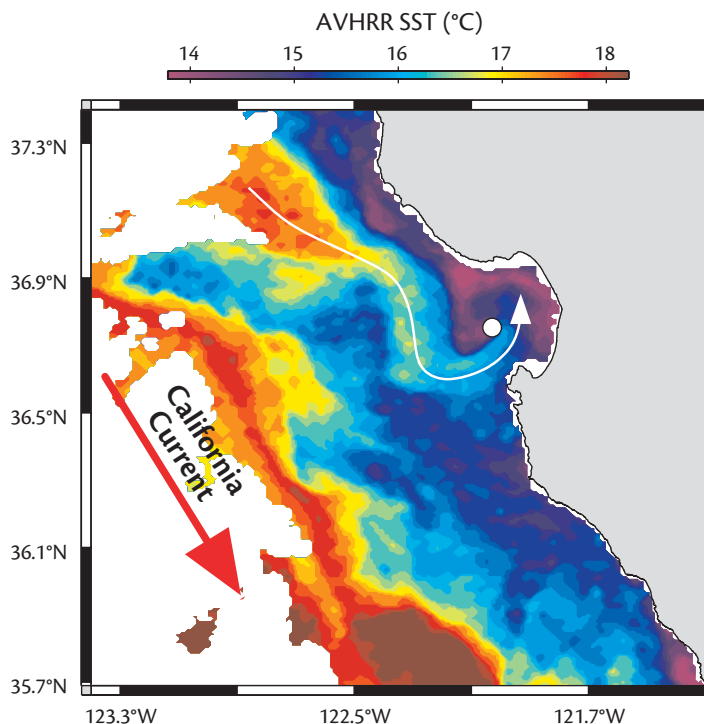


Figure 2. This Advanced Very High Resolution Radiometer (AVHRR) sea surface temperature (SST) image from September 29, 2002 (cf Figure 1C) illustrates a warm filament of the California Current involved in the rapid environmental changes preceding the red tide bloom in Monterey Bay. The filament is emphasized by the white curved line. The circle at the mouth of Monterey Bay shows the location of a mooring that provided measurements of water properties and ocean current velocities (Figure 3).

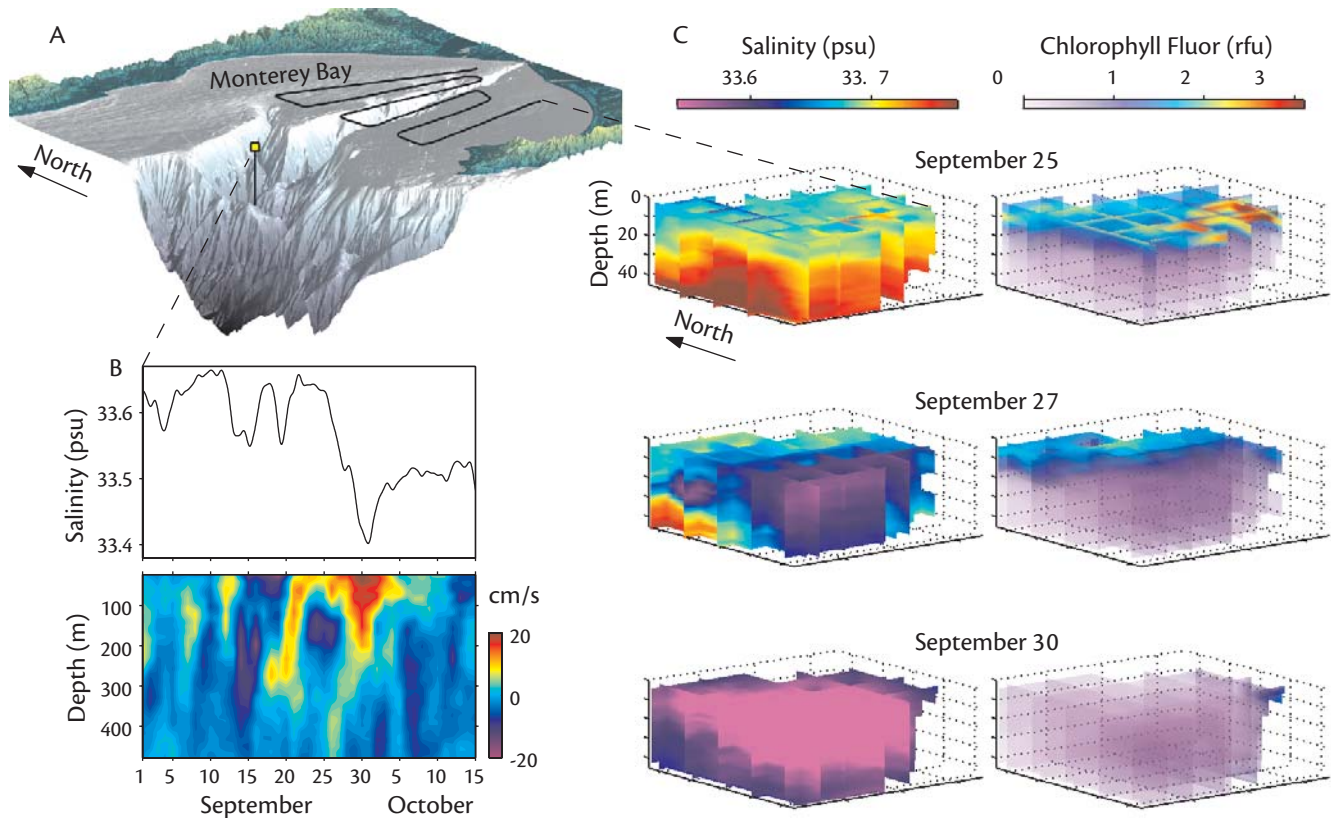


Figure 3. Monterey Bay was closely monitored *in situ* through the period of rapid change preceding the red tide. Measurement locations shown within the context of Monterey Bay coastal and seafloor topography (A) also provide viewpoint reference for the volume views in C. A mooring at the mouth of the bay captured the low salinity and enhanced flow signatures of intruding offshore waters (B). Salinity is the average of measurements at 1, 10, 20, 40 and 60 m; psu = practical salinity units. Meridional ocean current velocity is positive northward. While the mooring observations detailed conditions at the mouth of the bay, the bay interior was thoroughly surveyed by towed undulating vehicle along the winding track shown in A. The volume views (C) show salinity and chlorophyll fluorescence (representing phytoplankton abundance) within the monitored volume (rfu = relative fluorescence units; 1 rfu = 1 volt of fluorometer output voltage). Viewpoint is from above, southwest of the volume, as in A. Dramatic reduction in phytoplankton abundance (cf Figure 1) was evident throughout most of the bay.

Ship-Based Sensing

To monitor physical and bio-optical conditions through a large volume of Monterey Bay during September and October 2002, the R/V *Zephyr* regularly surveyed an 83-km, winding transect (Figure 3A), along which was towed a Sea Sciences Acrobat Model LTV-50 computer-controlled, undulating vehicle. Instrumentation included a Falmouth Scientific

Micro-CTD (conductivity, temperature, depth), a SeaTech light scattering sensor, and a WET Labs WETStar fluorometer. The depth range sampled was between ~3 and 50 m; the average number of profiles for full-volume surveys was 170; a full survey required ~7 hours. To represent properties within the volume, a three-dimensional interpolation of the sampled volume was created for each

measured variable via Delaunay triangulation in MATLAB. Density was calculated from temperature, salinity, and pressure using the UNESCO 1983 polynomial (Fofonoff and Millard, 1983). To compute average vertical density stratification from the volume surveys (Figure 4), density was binned to 1-m vertical resolution and vertical-density gradients (kg/m^3 per meter) were computed along

track for the complete survey. These were then averaged within density-range bins rather than depth bins because isopycnal depths varied across the survey domain. During the red tide bloom, sampling of phytoplankton was achieved on multiple days from the R/V *Zephyr* and the R/V *Point Sur*.

Autonomous Moored Sensing

Moorings of the Monterey Ocean Observing System at the mouth of Monterey Bay (Figure 3A) and 35 km further offshore provided measurements of temperature and salinity at multiple depths in the upper water column and ocean-current velocities between 20 and 500 m. Sea-Bird MicroCAT CTD instruments measured temperature and salinity, and RDI Workhorse Long-Ranger Acoustic Doppler Current Profilers measured water velocities. October 7 average current velocity at 20 m, shown in Figure 5A, was computed from the hourly time series that was first low-pass filtered with a 33-hour cutoff to remove tidal variation.

MULTI-SCALE PHYSICAL FORCING

Flushing of Monterey Bay

The core of the California Current (CC) is normally more than 100 km seaward of the central Monterey Bay coast (Collins et al., 2003). Direct influence of this boundary current on nearshore waters can occur in association with onshore flows during wind relaxation and in CC meanders and filaments. During late September 2002, a filament of the CC flowed into Monterey Bay and displaced resident bay waters. Intruding waters were relatively chlorophyll-poor (Figure 1B-D)

and warm (Figure 2). Continuous monitoring from a mooring at the mouth of Monterey Bay (Figure 3A) showed relatively low salinity and enhanced flow of the intruding waters (Figure 3B). A mooring 35 km further offshore detected low salinity and onshore flow anomalies associated with the CC variability.

We closely monitored the rapid physical and biological changes forced by the CC intrusion through much of Monterey Bay (Figure 3A, C). We observed unperturbed conditions, with phytoplankton abundant in the shallow sunlit waters, on September 25. By September 27, productive waters of the southern bay were displaced by intruding waters having lower salinity and much lower chlorophyll concentrations. By September 30 the entire central bay was flushed by intruding waters.

Enhancement of Stratification

Stratification is a measure of the strength of vertical gradients in density. Enhanced stratification is a primary condition associated with blooming of red tide dinoflagellates (Ryther, 1955; Margalef et al., 1979; Smayda, 1997; Gentien et al., this issue; Kudela et al., this issue). Significant consequences for phytoplankton ecology and HABs result from inputs of freshwater and terrestrial materials that influence physical, chemical and biological conditions, including stratification, in many coastal environments (Glibert et al., this issue; Cembella et al., this issue). In oceanic waters away from local nutrient inputs that accompany buoyant riverine or estuarine flows, stratification separates resources that sustain phytoplankton: light that increases in intensity toward the surface, and nutri-

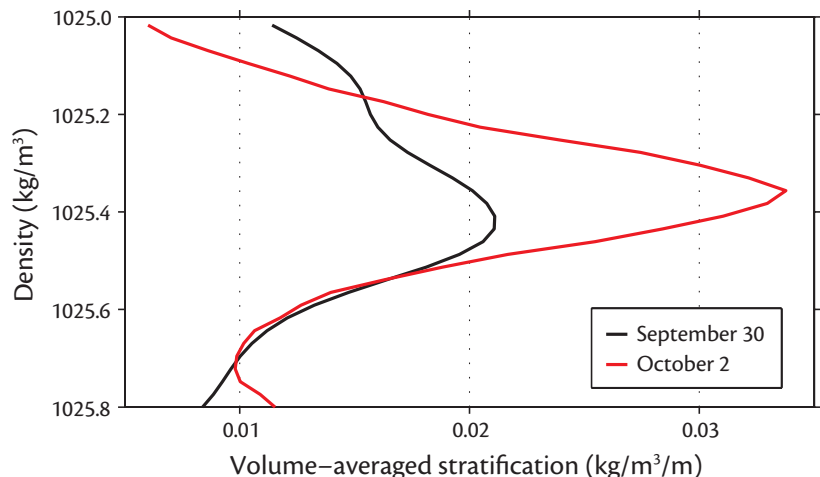


Figure 4. Profiles of the average vertical density gradient, computed from entire volume surveys (Figure 3C) show that stratification in Monterey Bay was strongly enhanced immediately preceding the red tide bloom. Because dinoflagellates are favored by stratification, this physical change was an important factor in the ensuing dinoflagellate red tide. Profiles were smoothed using a running-mean window of 0.08 kg/m³.

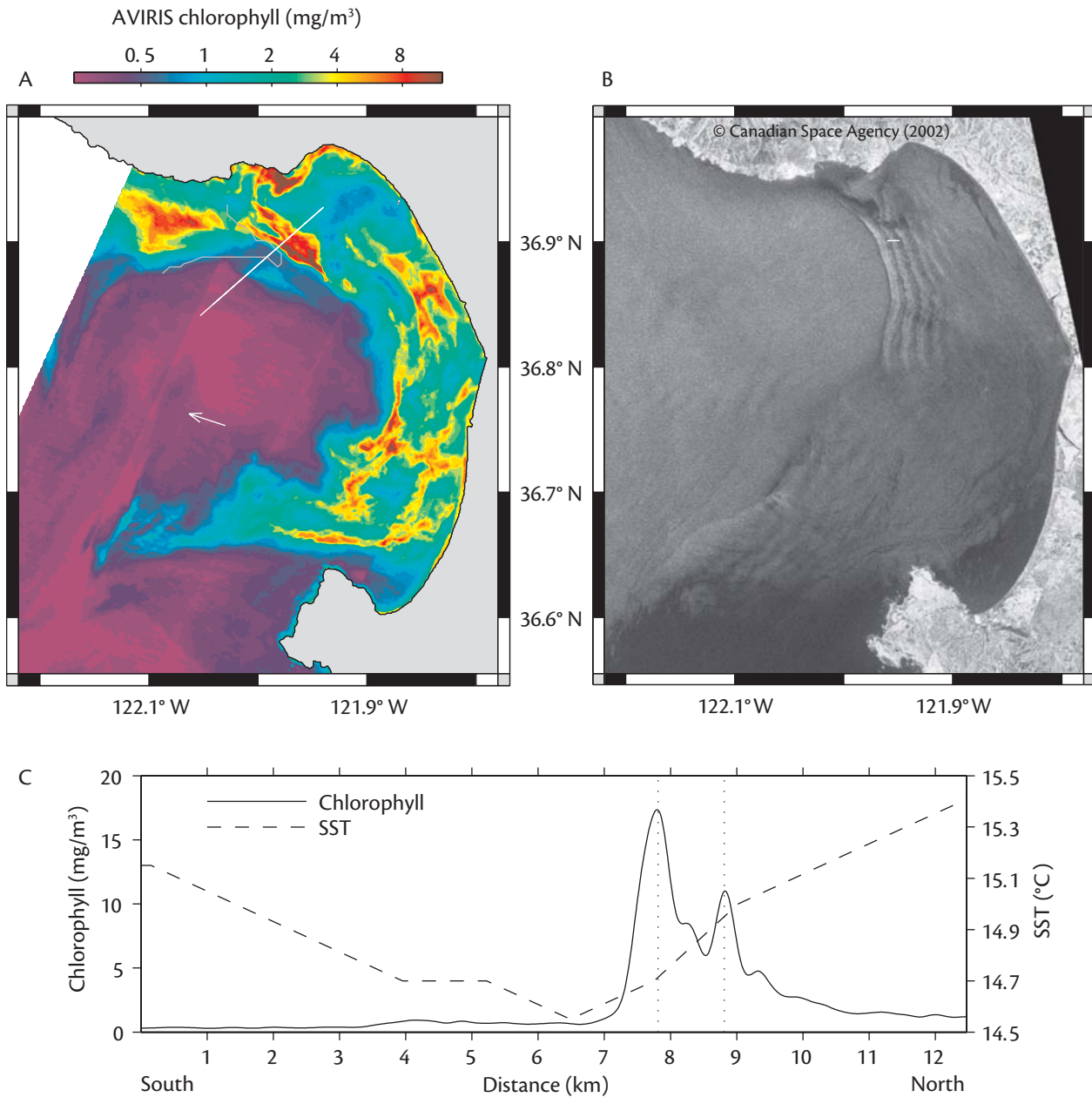


Figure 5. High-resolution, multidisciplinary remote sensing combined with *in situ* observations described physical processes involved in red tide spread and patchiness. The bloom spread clockwise around the bay (Figure 1). Clockwise wrapping of red tide waters around a low-chlorophyll anticyclone was pronounced in Airborne Visible/Infrared Imaging Spectrometer (AVIRIS) observations from October 7, 2002 (A). Image acquisition occurred between 21:01 and 21:52 GMT. Nearly concurrent SST (22:14 GMT) showed a cool filament flowing clockwise along the northern periphery of the anticyclone (the gray contour in A is the 14.6°C isotherm). Ocean current velocity measured at a mooring confirmed flow toward the northwest in the southwestern quadrant of the anticyclone (the white arrow represents October 7 average current velocity at 20 m depth; magnitude is 12.8 cm/s). Bloom patchiness was detailed by the high-resolution view of AVIRIS (A; more than 3000 times the resolution of the SeaWiFS imagery shown in Figure 1). Concentration of dinoflagellates in convergence zones was indicated at multiple scales, in association with confluence of water masses along the bloom periphery, and in wavelike aggregations having the scale of internal waves (IW) that propagated through the bloom. The IW signature of parallel dark-light bands was pronounced in the northern bay in same-day RADARSAT-1 synthetic aperture radar (SAR) imagery (B). SAR image acquisition began at 02:04 GMT, October 7, 2002; spatial resolution is ~30 m. The scale of 1 km was evident across the wave fronts (white scale bar along 36.9°N in B is 1 km) and in a transect of AVIRIS chlorophyll concentrations across a patch influenced by the IW. The transect location is shown in A, and chlorophyll concentrations are shown relative to AVHRR SST in C; the vertical dotted lines in C are 1 km apart. Chlorophyll peaks separated by 1 km were the dominant variation along the transect, and the chlorophyll transect was filtered to emphasize variation on scales > 0.5 km.

ents that increase in concentration with depth. By enabling access to separated light and nutrient resources, motility of dinoflagellates can provide competitive advantage over non-motile species under more strongly stratified conditions. Diminished turbulence associated with enhanced stratification may also minimize growth-retarding effects of turbulence on dinoflagellates (Smayda, 1997). Recent experiments, showing highly variable responses of dinoflagellate species to turbulence, identify this microscale physical forcing as an important research area for advancing understanding of red tides and HABs (Sullivan et al., 2003; Sullivan and Swift, 2003). Between September 30 (Figure 3C) and October 2, immediately preceding the red tide bloom, average stratification within the monitored volume increased sharply in the pycnocline, the vertical portion of the water column over which stratification is greatest (Figure 4). The increase, unrelated to local inputs of riverine or estuarine waters, established conditions advantageous for dinoflagellates.

Red Tide Inception and Spread

Shortly after the flushing and rapid stratification of the bay, the red tide bloom began in the northern bay, where the low-chlorophyll intruding waters met the remnants of resident high-chlorophyll bay waters (Figure 1D). From the northern bay, the bloom rapidly spread southward around the bay and out into the adjacent sea during October 3-8 (Figure 1E-G). An anticyclonic circulation pattern influencing bloom spread, as indicated by the satellite image sequence, was supported by high-resolution aircraft remote sensing of the bloom, satellite

SST imagery, and moored observations of ocean current velocity (Figure 5A). A circular region of low chlorophyll waters was centered at the mouth of the bay, and waters of the northern and southern bay wrapped clockwise around this feature. A cool SST filament extended from north-

ern Monterey Bay southeastward along the northern side of the anticyclone (gray contour in Figure 5A), indicating clockwise flow in northern bay waters. October 7 average near-surface velocity measured at the mooring confirmed northwestward flow in the southwestern quadrant of the anticyclone (arrow in Figure 5A) and is consistent with seaward extension of chlorophyll-rich waters from the southern bay.

Red Tide Patchiness

Red tides have long been considered paradigms of plankton patchiness (Ryther, 1955; Margalef et al., 1979). Interaction of ocean currents and plankton motility can create patchiness. Where horizontal flows converge and downwell, phytoplankton can be concentrated near the surface if they move upward at a rate greater than the downward flow of water. Positively buoyant diatoms form spectacular accumulations in convergence zones along large-scale wave fronts in the equatorial Pacific (Yoder et al., 1994). Having flagellar motility, dino-

flagellates can form dense aggregations near the surface by swimming upward against downward flows in convergence zones. *Ceratium furca* (Figure 1H) are strong swimmers with an exceptionally high ratio of swimming to sinking rate (Smayda, 2002). The ability of *C. furca*

**Ocean observing systems are critical for
advancing detection and prediction of
diverse marine phenomena (UNESCO, 2003).**

and *C. dens* to migrate against vertical currents has been observed off Baja California (Blasco, 1978).

Observing at more than 3000 times the spatial resolution of SeaWiFS satellite remote sensing, aircraft remote sensing of this red tide revealed a highly patchy distribution (Figure 5A). Airborne and satellite remote sensing support the influence of two physical processes on convergent flow patterns and bloom patchiness. The first was confluence of regional water masses along the seaward boundary of the bloom. A transect through the frontal zone and the center of a red tide patch (Figure 5A) shows a sharp increase of chlorophyll concentrations in the frontal zone where bloom waters converged with low chlorophyll waters of the anticyclone and the cool filament that flowed southeastward from the northern bay (between 7 and 8 km along-transect in Figure 5C). The second process was internal waves (IW), which create convergence zones that can concentrate phytoplankton (Franks, 1997). IW are evident in synthetic aperture ra-

dar (SAR) imagery because they modify ocean surface roughness in bands along the wave fronts (Thompson and Gaspárovic, 1986). A SAR image (Figure 5B) acquired 19 hours before the airborne remote sensing of the red tide revealed an IW packet in northern bay waters (parallel dark-light bands), including the region of the transected bloom patch. The white 1-km scale bar at 36.9°N defines an IW wavelength of ~1 km. The same scale was evident in chlorophyll concentrations along the transect, with the highest concentrations in two peaks separated by 1 km. The 19-hour offset in observation by the satellite radar and aircraft hyperspectral sensors would have introduced spatial offsets between IW and phytoplankton distributions due to wave propagation and movement of phytoplankton in ocean currents. However, the nearly parallel bands of high chlorophyll NW of the transect (Figure 5A) are also consistent with phytoplankton aggregation at the IW spatial scale, and these bands were orientated approximately parallel to the previously observed IW fronts. A SAR image taken 7 hours before the aircraft remote sens-

red tide initiation, growth, and spreading, frontal and IW forcing during the height of the red tide acted upon bloom biomass to create highly concentrated patches. Concentration of red tides and HABs influences not only the extent of surface water discoloration, but also the potential of the bloom to cause harm.

CONCLUDING REMARKS

Underlying initiation and development of this red tide in Monterey Bay were multiple physical phenomena occurring across a wide range of scales. Although we emphasize the importance of physical forcing, a possible biological factor is particularly relevant for *Ceratium* blooms: the effect of cell shape on grazing pressure. *Ceratium* species have horn-like processes that increase their maximum dimension (Figure 1H). It has been suggested that their horns could make them too large for small zooplankton grazers and difficult to handle and ingest for larger zooplankton (Nielson, 1990; Granéli et al., 1993; Teegarden et al., 2001). Reduced grazing pressure on *Ceratium* species could contribute to their blooming in Monterey Bay.

Because of their ecosystem, human, and economic impacts, red tides and HABs are important phenomena to detect and predict.

ing showed no evidence of IW in the region of this patch, thus it is possible that the wave-like aggregations retained an imprint of IW influence from the wave packet shown in Figure 5B.

While prior physical forcing involved

This research employed all primary techniques of ocean monitoring called for in the coastal module of the Global Ocean Observing System: remote sensing, *in situ* autonomous sensing, and discrete sampling followed by lab analysis

(UNESCO, 2003). Recent advancements in autonomous sensing are pivotal in enabling multidisciplinary observations at the spatial and temporal scales required to advance understanding and prediction of HABs (Babin et al., this issue). Integration of HAB research with ocean observing systems now being developed and applied is an important element of the national plan that will guide HAB research in the coming decade (Anderson and Ramsdell, this issue). Autonomous underwater vehicles (AUVs) are a key observing system component for augmenting the synoptic, multidisciplinary sensing that is required for phytoplankton ecology research, and AUVs are being routinely applied for these studies in Monterey Bay (Ryan et al., 2005). Ocean observing systems are critical for advancing detection and prediction of diverse marine phenomena (UNESCO, 2003). Because of their ecosystem, human, and economic impacts, red tides and HABs are important phenomena to detect and predict. Advancing predictive skill is dependent upon understanding the physical, chemical, and biological forcing underlying these complex phenomena.

ACKNOWLEDGEMENTS

This research was supported by the David and Lucile Packard Foundation, NASA grant NAG5-12692 and the Center for Integrated Marine Technologies through NOAA grant NAO16C2936. We thank the SeaWiFS Project and NASA/Goddard Distributed Active Archive Center for the production and distribution of the SeaWiFS imagery, the NASA AVIRIS Project for airborne image acquisition, and the Canadian Space Agency and the Alaska Satellite Facility for

production and distribution of the SAR imagery. M. Montes helped with AVIRIS atmospheric correction. Thanks to the Captain and crew of the R/V *Zephyr*, to L. Coletti, S. Fitzwater, H. Jannasch, and J. Plant for development, maintenance, and help in operation of the towed vehicle system, and to R. Marin for the photos of the red tide species in Figure 1. J.P.R. thanks P.J.S. Franks for discussion of patchiness and internal waves, and J. Yoder and T. Smayda for comments and suggestions on the manuscript. ☒

REFERENCES

- Anderson, D.M. 1995. Toxic red tides and harmful algal blooms: A practical challenge in coastal oceanography. *Reviews of Geophysics* 33(suppl.):1189-1200.
- Blasco, D. 1978. Observations on the diel migration of marine dinoflagellates of the Baja California coast. *Marine Biology* 46:41-47.
- Collins, C.A., J.T. Pennington, C.G. Castro, T.A. Rago, and F.P. Chavez. 2003. The California Current system off Monterey, California: Physical and biological coupling. *Deep-Sea Research Part II* 50:2389-2404.
- Donaghay, P.L. and T.R. Osborn. 1997. Toward a theory of biological-physical control of harmful algal bloom dynamics and impacts. *Limnology and Oceanography* 42:1283-1296.
- Fofonoff, N.P. and R.C. Millard. 1983. Algorithms for calculation of fundamental properties of seawater. *UNESCO Technical Papers in Marine Science*, No. 44. UNESCO, Paris, France, 53 pp.
- Franks, P.J.S. and D.M. Anderson. 1992. Alongshore transport of a toxic phytoplankton bloom in a buoyancy current: *Alexandrium tamarense* in the Gulf of Maine. *Marine Biology* 112:153-164.
- Franks, P.J.S. 1997. Spatial patterns in dense algal blooms. *Limnology and Oceanography* 42:1297-1305.
- Gao, B.C., M.J. Montes, Z. Ahmad, and C.O. Davis. 2000. Atmospheric correction algorithm for hyperspectral remote sensing of ocean color from space. *Applied Optics* 39:887-896.
- Granéli, E., P. Olsson, P. Carlsson, W. Granéli, and C. Nylander. 1993. Weak 'top-down' control of dinoflagellate growth in the coastal Skagerrak. *Journal of Plankton Research* 15:213-237.
- Hallegraeff, G.M. 2003. Harmful algal blooms: A global overview. Pp. 25-49 in *Manual on Harmful Marine Microalgae*, G.M. Hallegraeff, D.M. Anderson, and A.D. Cembella, eds. UNESCO, Paris, France.
- Horner, R.A., D.L. Garrison, and F.G. Plumley. 1997. Harmful algal blooms and red tide problems on the U.S. West coast. *Limnology and Oceanography* 42:1076-1088.
- Margalef, R., M. Estrada, and D. Blasco. 1979. Functional morphology of organisms involved in red tides, as adapted to decaying turbulence. Pp. 89-94 in *Toxic Dinoflagellate Blooms, Proceedings of the Second International Conference on toxic dinoflagellate blooms*, D.L. Taylor and H.H. Seliger, eds. Elsevier, New York, NY, USA.
- Montes, M.J., B-C Gao, and C.O. Davis. 2004. *NRL Atmospheric Correction Algorithms for Oceans: Tafkaa User's Guide*. NRL/MR/7230--04-8760. Naval Research Laboratory Washington, DC.
- Nielson, T.G. 1990. Contribution of zooplankton grazing in the decomposition of a *Ceratium* bloom. Collected Papers of the 1990 ICES Council Meeting. ICES, Copenhagen, Denmark, 33 pp.
- O'Reilly, J.E., S. Maritorena, B.G. Mitchell, D.A. Siegel, K.L. Carder, S.A. Garver, M. Kahru and C. McClain. 1998. Ocean color chlorophyll algorithms for SeaWiFS. *Journal of Geophysical Research* C103:24,937-24,953.
- Pitcher, G.C. and A.J. Boyd. 1996. Across-shelf and alongshore dinoflagellate distributions and the mechanisms of red tide formation within the southern Benguela upwelling system. Pp. 243-246 in *Harmful and Toxic Algal Blooms: Proceedings of the 7th International Conference on Toxic Phytoplankton*, T. Yasumoto, Y. Oshima and Y. Fukuyo, eds. UNESCO, Paris, France.
- Ryan, J.P., F.P. Chavez, and J.G. Bellingham. 2005. Physical-biological coupling in Monterey Bay, California: Topographic influences on phytoplankton ecology. *Marine Ecology Progress Series* 287:23-32.
- Ryther, J.H. 1955. Ecology of autotrophic marine dinoflagellates with reference to red water conditions. Pp. 387-414 in *The Luminescence of Biological Systems*, F.H. Johnson, ed. American Association for the Advancement of Science, Washington, D.C., USA.
- Ryther, J.H. 1969. Photosynthesis and fish production in the sea. *Science* 166:72-76.
- Smayda, T.J. 1997. Harmful algal blooms: Their ecophysiology and general relevance to phytoplankton blooms in the sea. *Limnology and Oceanography* 42:1137-1153.
- Smayda, T.J. 2000. Ecological features of harmful algal blooms in coastal upwelling systems. *South African Journal of Marine Science* 22:219-253.
- Smayda, T.J. 2002. Turbulence, watermass stratification and harmful algal blooms: An alternative view and frontal zones as pelagic seed banks. *Harmful Algae* 1:95-112.
- Sournia, A. 1995. Red-tide and toxic marine phytoplankton of the world ocean: an inquiry into biodiversity. Pp. 103-112 in *Harmful Marine Algal Blooms*, P. Lassus, G. Arzul, E. Erard-Le Denn, P. Gentien, and C. Marcaillou-LeBaut, eds. Lavoisier, Paris, France.
- Sullivan, J.M. and E. Swift. 2003. Effects of small-scale turbulence on net growth rate and size of ten species of marine dinoflagellates. *Journal of Phycology* 39:83-94.
- Sullivan, J.M., E. Swift, P.L. Donaghay, and J.E.B. Rines. 2003. Small-scale turbulence affects the division rate and morphology of two red-tide dinoflagellates. *Harmful Algae* 2:183-199.
- Teegarden G.J., R.G. Campbell, and E.G. Durbin. 2001. Zooplankton feeding behavior and particle selection in natural plankton assemblages containing toxic *Alexandrium* spp. *Marine Ecology Progress Series* 218:213-226.
- Tester, P.A., R.P. Stumpf, F.M. Vukovich, P.K. Fowler, and J.T. Turner. 1991. An expatriate red tide bloom: transport, distribution, and persistence. *Limnology and Oceanography* 36:1053-1061.
- Thompson, D.R. and R.F. Gasparovic. 1986. Intensity modulation in SAR images of internal waves. *Nature* 320:345-347.
- UNESCO. 2003. *The Integrated, Strategic Design Plan for the Coastal Oceans Observation Module of the Global Ocean Observing System*. GOOS Report No. 125. IOC Information Documents Series No. 1183. UNESCO, Paris, France, 190 pp.
- Yoder, J.A., S.G. Ackleson, R.T. Barber, P. Flament, and W.M. Balch. 1994. A line in the sea. *Nature* 371:689-692.

Advancing predictive skill is dependent upon understanding the physical, chemical, and biological forcing underlying these complex phenomena.